Accepted Manuscript

A generalized disjunctive programming framework for the optimal synthesis and analysis of processes for ethanol production from corn stover

Felipe Scott, Germán Aroca, José Antonio Caballero, Raúl Conejeros

Please cite this article as: Scott, F., Aroca, G., Caballero, J.A., Conejeros, R., A generalized disjunctive programming framework for the optimal synthesis and analysis of processes for ethanol production from corn stover, *Bioresource Technology* (2017), doi: http://dx.doi.org/10.1016/j.biortech.2017.03.180

A generalized disjunctive programming framework for the optimal synthesis and analysis of processes for ethanol production from corn stover

Felipe Scott[a,b,*,†], Germán Aroca[a,b], José Antonio Caballero[c], Raúl Conejeros[a,b].

[a] School of Biochemical Engineering, Pontificia Universidad Católica de Valparaíso, Av. Brasil 2085, Valparaíso, Chile

[b] Bioenercel S.A. Barrio Universitario s/n, Ideaincuba building, Concepción. Chile

[c] Department of Chemical Engineering, University of Alicante, Ap Correos 99, 03080. Alicante, Spain

Abstract

The aim of this study is to analyze the techno-economic performance of process configurations for ethanol production involving solid-liquid separators and reactors in the saccharification and fermentation stage, a family of process configurations where few alternatives have been proposed. Since including these process alternatives creates a large number of possible process configurations, a framework for process synthesis and optimization is proposed. This approach is supported on kinetic models fed with experimental data and a plant-wide techno-economic model. Among 150 process configurations, 40 show an improved MESP compared to a well-documented base case (BC), almost all include solid separators and some show energy retrieved in products 32% higher compared to the BC. Moreover, 16 of them also show a lower capital investment per unit of ethanol produced per year. Several of the process configurations found in this work have not been reported in the literature.

Keywords: Solid-liquid separation; Biofuels; Techno-economic analysis; Process optimization

1 Introduction

With an increasing concern about global warming and long-term sustainability of fossil fuels and chemicals, products obtained from lignocellulosic biomass have been intensively studied during the last decades as sustainable substitutes to petroleum based products (Dale et al., 2014). Lignocellulosic ethanol is the first biofuel produced from lignocellulosic materials instead of edible feedstock (Dale, 2015), an advance made possible by extensive research and development,

an existing infrastructure for ethanol distribution and use in some countries, and national renewable fuel policies and subsidies such as the Renewable Fuel Standard in the United States (Whistance et al., 2017). However, there is room for improvement, as much as the one observed in the evolution of the first petroleum refineries into the modern ones. A large effort has been made by the Process System Engineering community to develop decision-making tools based on optimization to select among the myriad of feedstock, technologies, processes and product alternatives. These efforts include optimization of the entire manufacturing system, including supply chain design and analysis (Giarola et al., 2012; Osmani and Zhang, 2014; You et al., 2012), selection of optimal processing plants including feedstock and products (Tsakalova et al., 2015) and individual plant sections and technologies (Gabriel and El-Halwagi, 2013; Matthews et al., 2015).

However, the current industry of ethanol production from corn stover requires an analysis focused at the equipment level to retrofit its existing ethanol plants and to design more sustainable (both economically and environmentally) new ones. In this regard, previous studies on improving the economics of lignocellulosic ethanol production generally fix the topology (this is the combination of processes, equipment and their interconnection) to analyze one process configuration at a time. For every topology, heat and mass balances are calculated using a process simulation software and an economic analysis is carried out to calculate a minimum product selling price, net present value or any other financial metric. In this way, some of the leading pretreatments for agricultural biomass have been analyzed in a techno economic study (Tao et al., 2011) showing that, despite significant variation in investments, the minimum product selling price varies little between the pretreatments. Moreover, several process configurations for the saccharification and fermentation of pretreated corn stover (PCS) have been analyzed, and in some cases compared, including separated saccharification and fermentation, SHF, and

2

simultaneous saccharification and fermentation, SSF (Bura et al., 2007; Saha et al., 2011). More advanced processing alternatives include separate processing of pulp and pretreatment liquor (Dutta et al., 2009) and several highly integrated bioprocesses, such as consolidated bioprocessing (CBP) where enzyme production, saccharification and fermentation are integrated into one system (Brethauer and Studer, 2014). However, a thorough comparison between process configurations is not possible due to an inexistent common framework of economic parameters and pretreatment conditions. Using the Attainable Region concept, Scott et al. (2013) showed that for the saccharification and fermentation of PCS the reactor networks that minimize the residence time can be constructed using plug flow reactors and continuously stirred tank reactors, despite the complexity of the reaction networks and underlying kinetics. However, no solid separators were included in this analysis. Including multiple reactors and solids separators in the saccharification and fermentation areas creates a combinatorial process synthesis problem, which calls for an optimization approach to determine the best process configurations from an economic perspective. Solid separators can be used to remove the unhydrolyzed cellulose and hemicellulose, allowing the separated fermentation of the released sugars. Thus, after combining the cell-free fermentation liquor with the separated solids, saccharification can resume with a reduced concentration of glucose and xylose. Although this alleviates product inhibition over the enzymatic reactions rates (Hodge et al., 2008; Teugjas and Väljamäe, 2013), the use of solid separators increases the investment costs, thus creating a new trade-off in the superstructure. This trade-off, have been recognized in the open literature (Sievers et al., 2014; Tao et al., 2012), however, no attempts have been made to analyze the optimal sequence of separation-reactor units in the saccharification and fermentation stages. This paper aims at filling this gap in the techno-economic analysis of process configurations in the saccharification and fermentation stages of a second generation ethanol plant using corn stover, through proposing and comparing process configurations beyond the conventional SHF, SSF and CBP processes by incorporating solid

separators. We propose a systematic, optimization-driven, framework for the search of economically improved process configurations (modeled at the equipment level) of a stand-alone and energy self-sufficient plant producing ethanol, electricity and solid fuel from corn stover. Recognizing that a unique (optimal) solution is uninformative for decision makers, optimal and suboptimal process configurations will be ranked.

The novelty of this work is twofold. Firstly, a framework for the synthesis of processes producing ethanol from corn stover, able to handle a mathematical representation of the superstructure and to compare it against a rigorous process simulation is presented. This framework allows the assessment of a large number of process configurations in a common technical and economic basis, or the optimization of the superstructure to find a process configuration with optimal economic performance. The methodology used to create the superstructure results in a more compact formulation compared to previously reported ones based on Mixed Integer non-linear Problem formulations (MINLP) (Baliban et al., 2013; Martín, 2016), a reduced computational burden and a more natural modeling approach. Secondly, its application produced several new process configurations for ethanol production from corn stover, which have not been reported in the literature and show improved Minimum Ethanol Selling Price (*MESP*) values respect to a benchmark.

2 Materials and Methods

This section introduces the Generalized Disjunctive Programming (GDP) formulation and the construction of the superstructure, this is, the mathematical representation of the process alternatives embedded in a plant-wide model. It is organized as follows. The problem is formally stated in Section 2.1, the conceptual design of the superstructure is presented in Section 2.2 and its mathematical representation is given in section 2.3 along with the optimization problems that will be solved to find process configurations with improved *MESP*. Finally, in Section 2.4 the

4

implementation of the problem is given, including the calibration of the superstructure against a rigorous simulation in Aspen HYSYS[TM].

2.1 *Problem statement*

The problem addressed by this framework can be formally stated as follows (equations are deferred to the Electronic Supplementary Information, ESI). Given is a superstructure for ethanol production from corn stover; this is, a mathematical representation of the pretreatment, saccharification, fermentation, distillation, combined heat and power production (CHP) and wastewater treatment (WWT) stages. Every plant design uses dilute sulfuric acid pretreatment and must be energy self-sufficient; generating heat and power from the lignin rich subproduct obtained after enzymatic hydrolysis, without consumption of gas, coal or oil. At the fermentation and saccharification stages, a number of process alternatives (equipment) are available to be included. They are represented by saccharification reactors, fermentation reactors and solid separators. Properly arranged, a combination of process alternatives can represent well-known process configurations, such as SHF or SSF, or new ones, including processes using pulp separation and cell recycle. The saccharification and fermentation reactors include consistent experimental information captured in the form of kinetic models, while pulp separators incorporate operational information generated using PCS. Investment and operating costs for every operation in the superstructure are also included. Hence, the linear and nonlinear equations in the superstructure allow for the calculation of process economics for any of the complete lignocellulosic ethanol production plants embedded in the superstructure.

The objective is to minimize the *MESP* (see Section 2.2.3) by optimizing the process design variables, operating variables and process topology (which process alternatives will be included in a given biomass to ethanol process). Reactors volume, solid separator areas, CHP installed capacity, areas of heat exchangers and height and diameter of distillation columns among others,

represent the design variables. Operating variables include enzyme dosage, reactors temperature and solid fraction, washing efficiency in solid separators and boiler operating pressure.

2.2 *Ethanol process superstructure: conceptual design*

This section outlines the design considerations, modeling approach and sources of information used to build the superstructure of processes for ethanol production from corn stover. Details regarding the mathematical model are shown in the ESI.

2.2.1 *Plant capacity, base case and substrate*

The base case corresponds to the biochemical ethanol conversion process proposed by NREL (Humbird et al., 2011). Corn stover is pretreated using a mild thermochemical pretreatment, followed by liquefaction and SSF. As in the base case, plant capacity was set at 2000 metric ton of dry corn stover (oven dry metric ton, ODMT) per day. The pretreatment stage for every process configuration, and not only the base case, follows the design and operating conditions indicated in the NREL report (Humbird et al., 2011). Thus, capital and operating expenditures were taken from the aforementioned study for this stage. Moreover, since the operating conditions in the pretreatment are fixed, so is the pretreated substrate composition.

2.2.2 *Process superstructure modeling*

Detailed models for the saccharification and fermentation, product recovery, CHP and WWT stages were created. Since product recovery and WWT stages were modified from the base case, only the description of the saccharification and fermentation stage is presented in this section. Moreover, the CHP stage was adapted from the base case by allowing that a fraction of the separated solids (subject to optimization) can be allocated for pellet production. The process considers drying, pelletization and pellet storage. Technical and economic parameters for this section were taken from literature (Thek and Obernberger, 2004). A thorough description of these stages is presented in the ESI. The saccharification and fermentation stage was modelled as an interconnected network of continuous reactors, pulp separators and cell separators (Figure 1).

6

Saccharification reactors ($R1_A$, $R2_A$ and $R3_A$) were modeled as continuous stirred tank reactors where cellulose is converted to cellobiose and glucose. These reactors are operated with a residence time greater than 24 h, producing cellulose conversions typically greater than 20%; this is, 20% of the cellulose in the feed stream is converted to glucose and cellobiose. At the insoluble solids fractions selected by the optimization framework, this conversion was deemed enough as to guarantee that its content behaves as a pourable fluid with yield stresses less than 10 Pa (Roche et al., 2009; Stickel et al., 2009). Reaction stoichiometry and rates were taken from Scott et al. (2015). This model was selected because it considers solid contents between 10 to 25% *w/w*, washed or unwashed solids, the effect of enzyme loading over cellulose conversion and a pretreated substrate consistent with the one included in the superstructure (dilute sulfuric acid pretreated corn-stover at NREL pilot plant). Moreover, when combined with operating and capital costs equations, this model is able to capture the trade-off between the increasing conversion and the higher expenditures in enzymes when the enzyme dosage in the saccharification stage is increased. Once embedded in the mathematical model of the superstructure, the enzymatic hydrolysis model can be used to select an optimal solid loading and enzyme dose that minimizes product cost for each process configuration.

Sugars released by the saccharification of cellulose and the sugars contained in the pretreatment liquor can be fermented using *S. cerevisiae*, able to transform glucose to ethanol, or a recombinant *Z. mobilis*, capable of fermenting xylose and glucose. Fermentation with *S. cerevisiae* was modeled according to Rivera et al. (2006), accounting for the effects of temperature and sugar concentration over reaction rates, while fermentation with *Z. mobilis* ZM4(pZB5) was described by the kinetic expressions presented by Leksawasdi et al. (2001), at a fixed temperature of 30 °C. Thus, when *S. cerevisiae* is used, the temperature during SSF is an optimization variable since higher temperatures, with a maximum of 40°C, increase enzymatic

7

hydrolysis rates but affect cells growth and ethanol yield. Reactors included in the superstructure allow for multiple fermentation alternatives. Reactors $R1_B$, $R2_B$ and $R3_B$ can operate in SSF mode or in fermentation mode (pulp-free) and with either *S. cerevisiae* or *Z. mobilis*. On the other hand, reactors $RC5_1$ and $RC5_2$ are only allowed to operate using *Z. mobilis* (see Figure 1).

Vacuum belt filters were selected for the separation of PCS solids, as they represent the most cost effective option for this task (Sievers et al., 2014). Two class of separators were included in the superstructure (Figure 1): separators SS-LE1 and SS-LE2 do not include washing, but can process 100 kg $h^{-1}m^{-2}$ of insoluble solids, and separators SS-HE0 to SS-HE3, that on the contrary, produce washed solids, increasing sugars recovery, but they have a reduced throughput of 60 kg $h^{-1}m^{-2}$. The wash ratio (wash water volumes passed through the cake) is subject to optimization since this variable controls the sugars recovery efficiency according to the correlation presented by Sievers et al. (2014) for PCS.

2.2.3 *Economic assessment and objective function*

The objective function for the optimization problem corresponds to the *MESP* based on annualized costs. This indicator incorporates the total investment cost, operating costs and ethanol and coproduct sales, allowing a fair comparison of the process configurations included in the superstructure. As shown in Eq. 1, the *MESP* corresponds to the minimum plant-gate selling price of ethanol (in USD per kg) allowing a zero-annualized cost, this considering that 60 % of investment is financed using a 10-year bank loan at 8% interest rate and the remaining 40% is financed by equity at a 10% rate. These conditions were selected to resemble the base case and produce a capital charge factor (f_a) equal to 0.131 (Humbird et al., 2011).

$$MESP_a = \{x: F_E x + P_E E + P_P P - OPEX - f_a TCI = 0\}$$ Eq. 1

Purchased equipment costs were estimated using the cost correlations presented in ESI (section S1 1.7) and a factored approach in which multipliers are applied to the sum of purchased

equipment costs allows the estimation of the total capital investment (TCI). More details can be found in the ESI (section S1 1.7). All capital costs were converted to 2007 USD using the Chemical Engineering Plant Cost Index to be comparable to the base case. The operating cost (OPEX) was estimated from the mass and energy balances and the prices and costs of enzymes (4.24 USD/kg of protein for cellulose and β-glucosidase), corn stover (64.5 USD per dry metric ton), chemicals and salaries as in the base case. Coproduct sales are represented by electricity (E, in MWh$_e$/y, 55.2 USD/MWh) and pellets (P, in MWh$_t$/y, 22.5 USD/MWh), whose price is assumed to be determined by its energy content and considers its transportation costs (Argus Biomass Markets, 2015). Maintenance and insurance were taken as 3% and 0.7% of the capital investment, respectively.

2.3 *Mathematical modeling of the process superstructure*

In this work, a GDP formulation is used to create a framework to find economically improved process configurations for the production of ethanol from corn stover. GDP characterize problems in terms of Boolean and continuous variables, allowing the representation of process alternatives as disjunctions (Grossmann and Ruiz, 2012) as in equation GDP-1. The set of Boolean variables Y_k indicates whether a disjunction D_k (with $k = 1,..,28$) is active or inactive. If true, all the equations within the disjunction representing mass and energy balances, investment and operational costs, and physical and chemical equilibrium for a particular piece of equipment and its connections will be included in the superstructure. If the Boolean variable is false, the disjunction is inactive and the constraints within it are ignored. Thus, Boolean variables control whether a reactor or separator is included in a process.

$$\min_{x,Y_k} MESP \qquad \text{(GDP-1)}$$
$$s.t. \ h(x) = 0$$
$$g(x) \leq 0$$

9

$$\begin{bmatrix} Y_k \\ r_k(x) \le 0 \\ s_k(x) = 0 \end{bmatrix} \vee \begin{bmatrix} \neg Y_k \\ x_{i,k} = 0 \end{bmatrix} \quad k \in K$$

$$\Omega(Y) = True$$

$$x^{lo} \le x \le x^{up},$$

$$x_{i,k} \subseteq x, x \in \mathbb{R}^n, Y_k \in \{True, False\}, k \in K$$

In problem GDP-1, x is a vector of mass and energy flows, temperatures, pressures, enzyme dosages, capital and operating costs and any other continuous variable. Constraints that are always active (they do not belong to any disjunction) are represented by h and g, corresponding to mass and energy balances, design and costing equations for the pretreatment, distillation, CHP and WWT areas. On the other hand, r_k and s_k denote equations that are incorporated to the problem if and only if the disjunction they belong is active ($Y_k = True$), controlled by a set of Boolean variables Y_k. Otherwise, when $Y_k = False$, the corresponding constraints are ignored.

In combination with the Logic-based Outer Approximation algorithm (Türkay and Grossmann, 1996), the GDP formulation shown in equation GDP-1 allows avoiding the reformulation of the problem as an MINLP. Thereby, no relaxed problems need to be solved, but only a set of sub-problems that corresponds to feasible process configurations. Moreover, variables and constraints related to non-active disjunctions are not included in the optimization problems, hence, difficulties related to errors in function evaluations are avoided and the size of the non-linear problems (NLP) is reduced because only the equations in the active disjunctions are included in each problem. Other advantages of the GDP formulation can be found elsewhere (Navarro-Amorós et al., 2014). Thus, the use of GDP in the framework presented in this work allows for a more natural modeling approach of the alternatives embedded in the superstructure and a more efficient optimization as compared with a traditional MINLP formulation.

A set of active disjunctions selected in such a way that the feed stream to the saccharification and fermentation section (F300) is converted to ethanol is a valid selection, more properly, they

define a *feasible topology* for the process flowsheet. For example, the saccharification and fermentation stages of the base case scenario are represented by the process flowsheet where $Y_j = True, j \in \{1,3,8,10,16,21,25\}$, and all the remaining disjunctions are false. From Figure 1, the process starts with $F300$ being fed to $R1_A$ (D_{25} is active) after ammonia conditioning, the stream leaving $R1_A$ is transferred to $R1_B$ (D_3 and D_1 are active) and its outlet stream feds $R2_B$ (D_8 and D_{10} are active). Finally, the outlet stream from $R2_B$ is fed to $R3_B$ (D_{16} is active) and the product stream, the stream leaving $R3_B$ since D_{21} is active, is sent to the distillation area.

Since a large number of the conceivable process configurations that can be obtained from the 2^{28} possible combinations of the Boolean variables will not define feasible topologies, it is necessary to introduce a set of logic propositions relating the Boolean variables ($\mathbf{\Omega}(\mathbf{Y}) = True$). Logic arguments can be incorporated to the superstructure by using the logical operators OR ($\vee$), AND ($\wedge$), IF-THEN ($\Rightarrow$), XOR (exclusive or, $\underline{\vee}$), NOT ($\neg$) and IF AND ONLY IF ($\Leftrightarrow$). For example, in Figure 1, stream $F300$ can be fed to SS-HE0 (D_{22} is active) or be directly fed to $R1_A$ (D_{25} is active), but both alternatives cannot be simultaneously selected. This logic argument can be represented as $Y_{22} \underline{\vee} Y_{25}$. A list of the logical propositions included in the superstructure is presented in the ESI (section S1). The set of logic propositions $\mathbf{\Omega}(\mathbf{Y}) = True$, can be converted to a set of linear equations with binary variables ($\mathbf{E}\mathbf{y} \leq \mathbf{e}$) by replacing each Boolean variable by a binary one, representing each proposition in its conjunctive normal form and, finally, transforming logic propositions to linear constraints using Boolean algebra rules (Williams, 1999). The list of feasible process configurations can be found by iteratively solving the MILP: $\min\{\mathbf{c}\mathbf{y} \mid \mathbf{E}\mathbf{y} \leq \mathbf{e}, \mathbf{y} \in \{0,1\}\}$, and augmenting it with a binary cut on each iteration to exclude the previously found solution for the binary variables (Raman and Grossmann, 1991). The list of the 150 feasible process configurations is presented in the ESI (section S2). Each entry in the list

represents a process configuration whose process flow diagram in the saccharification and fermentation stages can be traced by following the active disjunctions in Figure 1.

Before introducing the use of the GDP formulation to obtain optimal process configurations a remark is made. If a valid process configuration is selected, then Y is no longer subject to optimization, thus eliminating the binary variables from the optimization problem converting it to an NLP.

2.3.1   *Minimum MESP processes: optimization of the superstructure and the base case scenario.*

The most profitable process configurations in the superstructure can be identified by solving problem GDP-1or by non-linear optimization (NLP) of each one of the feasible process configurations (fixing the process configurations beforehand). The superstructure includes 150 valid process configurations, including the base case process configuration. They can be operated with recombinant *Z. mobilis* in every fermenter or with *S. cerevisiae* in reactors $R1_B$ to $R3_B$ and *Z. mobilis* in reactors $RC5_1$ and $RC5_2$, thus creating two scenarios. Thereby, 300 processes need to be optimized by solving each NLP one at a time. Alternatively, the optimal process configuration can be found by solving problem GDP-P1. The complete GDP-1 problem includes 28 Boolean variables, 3063 continuous variables, 1069 non-linear equations, 1758 linear equations and 52 logic equations.

To analyze the techno economic performance of the process configurations in the superstructure, first, the MESP of the base case process configuration is calculated using the operating conditions reported by Humbird et al. (2011). To provide a fair comparison, in a second stage of optimization, the operating variables of the base case process configuration are allowed to be optimized; including enzyme dosing, temperature and solid fraction in saccharification reactors, thus defining an Optimized Base Case (OBC). Finally, the remaining 149 process

configurations in the superstructure are benchmarked against the OBC in the two aforementioned scenarios.

Solving GDP-1 directly allows the identification of the optimal process configuration, given that it is possible to calculate the global optima of this problem, or a near optimal configuration in a time that will generally be shorter than visiting every process configuration, and that in the worst case, will be the same. However, if the designer is not interested in only the "best" solution but rather in a list of processes ordered according to its *MESP* value, problem GDP-1 needs to be solved iteratively augmenting it on each iteration with an integer constraint that eliminates the previously found process configuration from the superstructure. Thus, depending on the number of elements in the list that the designer wants to find, and the number of possible process configurations in the superstructure, it might be less time consuming to optimize each process configuration and store the value of the design and operating variables. The last approach is facilitated in a GDP framework, where each NLP can be constructed automatically from the superstructure including only the relevant equations and variables, thus limiting the size of the problem.

2.4 *Implementation*

2.4.1 *Problem solution*

The optimization problem GDP-1, the backbone of the framework presented in this work, was solved using the Logic-based Outer Approximation algorithm to exploit the structure of the Generalized Disjunctive Programing approach taken in this framework (Navarro-Amorós et al., 2014; Türkay and Grossmann, 1996). Since some constraints in GDP-1 are non-convex, the global optimality of the solution cannot be guaranteed.

The set of linear and non-linear equations representing the superstructure was implemented in MATLAB^{TM} using an in-house language tailored for GDP problems. The file with the problem

definition is processed and transformed into a standard NLP problem or MILP problem using

OPTI, a toolbox for MATLAB[TM] (Currie and Wilson, 2012). The generated NLP problems were

solved using GAMS[TM], CONOPT (Drud, 1985) or IPOPT (Wächter and Biegler, 2006) while

CPLEX was used to obtain the solution of the MILP master problems.

2.4.2 Calibration of the superstructure

The superstructure was calibrated against a rigorous simulation in Aspen HYSYS[TM] by

debugging involuntary errors in coding and adjusting the values of physical properties such as

densities and enthalpies to the values calculated by Aspen HYSYS[TM]. This was performed until a

close correlation between the values of key process indicators calculated by the superstructure, as

a set of linear and non-linear equations, matched the values calculated by the representation of

the superstructure in the process simulator. This comparison was made using a reduced number

of process configurations that were selected as to include every disjunction being active at least

once, thus ensuring that all the equipment and streams that can be included (or not) in a process

configuration are tested. This comparison was automatized using a connection between

MATLAB[TM] and Aspen HYSYS[TM] (Navarro-Amorós et al., 2014). Details regarding the

implementation of the superstructure can be found in section S3 of the supplementary material.

3   Results and discussion

In this section, the results for the optimal synthesis of processes for ethanol production from

corn stover are presented and discussed. In Subsections 3.1 the mathematical formulation of the

superstructure is compared with a rigorous formulation in HYSYS, showing that they produce

equivalent values for key process indicators. Next, in subsection 3.2 the operational variables in

the base case process configuration are optimized, producing a lower MESP value than the one

found using the conditions reported by Humbird et al. (2011). Finally, in subsection 3.3, every

14

process in the superstructure is optimized and compared (in terms of MESP) with the optimized base case.

3.1 *Comparison of rigorous process simulation in HYSYS and results from NLP*

Results are presented in Figure 2 A to D for cellulose conversion, ethanol yield, installed equipment cost for the saccharification and fermentation area and power consumption indicating a proper correlation between the values calculated by the process simulator and the simplified mathematical representation in the superstructure.

Figure 2.E shows the thermal energy (provided by saturated steam at 6 bar) required to achieve a 92.5% *w/w* ethanol content from a stream containing ethanol between 1 to 7% *w/w*. Three designs are compared, a design took from Humbird et al.(2011), Galbe et al.(2007) and the design used in this work. These designs were rigorously simulated in HYSYS to produce the result shown. It can be seen that the design used in this work requires less thermal energy because of its heat integrated scheme (see supplementary material) and that above 3 % *w/w* ethanol the thermal energy requirements decrease slightly compared to more diluted solutions. These results were used to establish a correlation between energy requirements for distillation and the ethanol mass fraction of the stream entering the concentration column. This correlation was used to avoid the rigorous modeling of the two columns distillation system in the superstructure using the MESH equations (Material, Equilibrium, Summation and Enthalpy). Figure 2.F shows the ethanol titers of the stream entering the concentration column for the 150 process configurations embedded in the superstructure for the scenario where *Z. mobilis* is used in every fermenter and also for the scenario where *S. cerevisiae* is used in $R1_B$ to $R3_B$. The ethanol titer produced in all process configurations range between 3.5 to 6.5% *w/w*, values in the zone where increasing ethanol contents have reduced impacts in the energy requirements for distillation according to Figure 2.E. However, a proportionality was found between ethanol titer and the percentage of

energy from corn stover retrieved as ethanol, electricity and pellets, whose values span from 44 to 62% (Figure 2.F).

3.2 *Base case process configuration.*

According to the technical report published by NREL (Humbird et al., 2011), the pulp at 10.6% *w/w* insoluble solids content is liquefied in a battery of continuous parallel reactors with a residence time of 24 h and an enzyme loading of 20 mg of protein per gram of glucan. The liquefied pulp is discharged to a battery of batch reactors where saccharification continues for 60 h at 48°C. Since the superstructure is a network of continuous reactors and pulp separators, the process configuration representing the base case is mimicked by the process configuration C146 (shown in **Figure 5**, panel OCB) where all reactors are operated in continuous mode. Using the same operating conditions as in the base case and not allowing the production of pellets from the enzymatic hydrolysis solid residue, an *MESP* of 69.1 cUSD/kg was calculated based on annualized costs. When a discounted cash flow rate of return analysis (DCFROR) is used to calculate the *MESP*, a value of 72,3 cUSD/kg was obtained, similar to the 71.9 cUSD kg^{-1} calculated by Humbird et al. (2011). An ethanol yield of 231 kg ODMT^{-1} and an ethanol volumetric productivity of 0.42 kg m^{-3}h^{-1} were calculated. These values compare with 260 kg ODMT^{-1} and 0.39 kg m^{-3}h^{-1} calculated from the work of Humbird et al. (2011). The specific capital investment per kg of ethanol produced per year and the amount of ethanol produced per unit mass of enzymes are shown in Figure 3 A and C. The difference in the specific capital investment values can be explained by the capital expenditures in enzyme production included by Humbird et al. (2011), an expenditure not included in the superstructure, where enzymes are assumed to be purchased. Thus, the process configuration mimicking the base case resembles the results obtained by Humbird et al. (2011). If the aforementioned values of the operating

16

conditions are allowed to be optimized, an *MESP* equal to 67.2 cUSD kg^{-1} is calculated by

reducing the enzyme dose to an optimal value of 10.4 mg g^{-1}, reducing the insoluble solids

fraction to 11.3% *w/w* and increasing the total residence time to 128 h. This *MESP* value is

guaranteed to be the optimal value for configuration C146 since the global NLP solver BARON

(Sahinidis, 1996) was used to check this result. These changes lead to an increase in the specific

capital investment, but also increase the specific ethanol production per mass of enzymes used

(see Figure 3 A and C). A simplified mass balance for the OBC is shown in **Figure 5** A.

3.3   *Optimization of the superstructure*

3.3.1   *Optimization of the superstructure using the logic-based outer approximation algorithm*

The optimal solution of problem GDP-1, including Boolean variables, identified by the

algorithm corresponds to C135 with an *MESP* of 61.68 cUSD kg^{-1}. The algorithm terminates at

NLP worsening. After solving each NLP subproblem in the superstructure (with *S. cerevisiae* in

R1$_B$ to R3$_B$, see the next section) the optimal solution of the superstructure corresponds to C145

(*MESP* of 61.62 cUSD kg^{-1}). For the scenario where *Z. mobilis* is used in every reactor in the

superstructure, the solution of the GDP-1 problem identified C133 as the optimal solution with an

MESP equal to 63.85 cUSD kg^{-1}. After solving every valid process configuration, the optimal

solution of the superstructure using *Z. mobilis* corresponds to C128 with an *MESP* of 62.41

cUSD kg^{-1}. As stated in section 2.4.1, the optimization method used to solve GDP-1 might

produce sub-optimal solutions due to the non-convexity of the problem. However, results show

that the GDP framework achieves near optimal process configurations.

3.3.2   *Optimization of each valid process configuration in the superstructure*

Since the direct solution of GDP-1 was shown to produce suboptimal process configurations,

it was decided to optimize the operating variables of each process configuration in the

superstructure. The NLP problems generated by this approach, are readily solved (within 3 minutes), thanks to the reduced number of variables and constraints obtained in this formulation.

Figure 3 shows the results for the 300 valid processes (150 process configurations in two scenarios) embedded in the superstructure. Each dot is the result of a non-linear optimization of the design and operating variables with fixed (but different) topology of the process. Figure 3 A shows that when *S. cerevisiae* is used in reactors $R1_B$ to $R3_B$ and xylose is not fermented to ethanol, only *MESPs* above one cUSD kg^{-1} are attained with specific total capital investments per kg of ethanol produced per year (TCI_{esp}) larger than 4 *USD/kg$_{EtOH}$*. These process configurations are characterized by disjunction 23 being active, hence the xylose-rich stream is separated and directed to biogas production, or disjunction 25 being active, and thereby xylose is not fermented arriving at the WWT area in the stillage stream (see Figure 1, D23 and D25). Figure 3.C presents a zoom of process configurations that achieve *MESP* values below 75 cUSD kg^{-1} in Figure 3.A. Every process configuration showing an *MESP* below the OBC includes solid separation of the pulp and liquor after the pretreatment reactor (D22 is active), and a number of these process configurations include an intermediate solid separator (D5 or D6 is active).

Altogether, and when *S. cerevisiae* is used in reactors $R1_B$ to $R3_B$ (when active), 26 process configurations show *MESP* values lower than the OBC and 11 of them show specific capital investments below the one shown by the OBC (Figure 3.C). Moreover, the specific ethanol production per mass of enzymes (P_{enz}^{EtOH}) used by these process configurations is larger than the values calculated for both the base case and its optimized version (Figure 3.E). This can be explained by the low optimal enzyme doses calculated for these process configurations, with values between 6.8 and 9.2 mg of protein per gram of glucan and higher ethanol yields.

18

When *Z. mobilis* is used in each fermenter, 14 process configurations show an improved *MESP* compared to the OBC, and 5 of them show specific capital investments below the one shown by the OBC (Figure 3 B, D and F). Process configurations where the stream rich in xylose separated after pretreatment is used for biogas production, instead of ethanol (D23 is active), show the worst *MESP*s. On the other hand, those processes showing *MESPs* below the OBC include separated fermentation of the xylose reach stream after solid separation (D24 is active), separation of pulp and liquor after liquefaction (either D5 or D6 is active) or processing of the pretreatment reactor outlet stream without separation. It is interesting to point out that the optimal process configuration when *Z. mobilis* is used corresponds to C128 (**Figure 5**.B), including pulp and liquor separation after the pretreatment reactor. Thus, although it would be simpler to simultaneously process both pulp and liquor in a train of reactors, the separated processing of pulp and the liquor rich in xylose allows a smaller *MESP* to be achieved. Despite the reduction in the specific capital investment achieved by process C128, the total capital investment for this process configuration at fixed plant capacity (2000 ODMT of corn stover per day) is higher than the value calculated for the OBC (345.8 MMUSD, see Table 1). Thus, the decrease in the specific capital investment is caused by a 9.5% increase in ethanol production per year in C128 as compared to the OBC. Thereby, if the same plant capacity (in terms of ethanol production per year) is to be achieved, selecting C128 as the process configuration will result in a smaller TCI than if the base case configuration is selected. In fact, after setting a new constraint that equals the ethanol production in C128 to 5.12 kg s^{-1} (as in the OBC) and performing a non-linear optimization, plant capacity is calculated as 1974 ODMT d^{-1}, achieving an *MESP* equal to 63.9 cUSD kg^{-1} and TCI equal to 343 MMUSD.

Figure 5 and Table 1 show mass balances, economic and process indicators for selected process configurations, including the OBC. As it can be seen from Table 1, the OBC shows the smaller

19

total capital investment. However, also achieves the lower ethanol production (see **Figure 5**) at a fixed plant capacity of 2000 ODMT d^{-1}. In turn, the lower total operating costs for C128, C145 and C69, promoted by a decrease in the expenditures in enzymes, and the higher ethanol yields translate in a lower payback time and *MESP* (calculated either using a DCFROR analysis (Humbird et al., 2011) or annualized costs) for these process configurations compared to the OBC. In terms of energy consumption, the OBC shows the smaller specific thermal energy consumption (provided by steam). This can be explained by its higher ethanol titer compared to other process configurations in Table 1. Since a higher amount of steam must be provided to the reboiler of the ethanol concentration column in these process configurations, the OBC also produces more electricity and can export a large amount of power to the grid. Another factor that determines a lower electricity production in process configurations different than the OBC is pellet production. However, the results from the nonlinear optimization of the design and operating variables show that in order to achieve optimal *MESPs*, a mix of ethanol, electricity and pellets must be produced. Moreover, producing pellets allows for more of the energy contained in corn stover to be included in products (Table 1). As a comparison, for the OBC, 38.0% and 8.9% of the energy in corn stover (based on the lower heating value from Humbird et al. (2011)) is retrieved as energy in ethanol and electricity. On the other hand, for process configuration C131, 40.5%, 4.1% and 13.1% of the energy in corn stover ends in ethanol, electricity and pellets. The maximum value of total energy in products was achieved by C111 reaching 62.4%, a 1.32-fold increase compared to the base case. In this analysis, no difference in the "quality" of the energy in each product was made. Certainly, liquid fuels, electricity and solid fuels are intended for different purposes, and so factors can be used to valuate the different forms of energy.

The difference between the *MESP* of the base case and the process with the lower *MESP* in the superstructure (C145) shows a 10.8% reduction. This result matches with other technical and

economic reports comparing similar processes for lignocellulosic ethanol production. Tao et al. (2011) compare processes based on leading pretreatment operations including dilute acid, AFEX, liquid hot water, soaking in aqueous ammonia (SAA), and sulfur dioxide-impregnated steam explosion (SO_2) for switchgrass processing. They found a 9% reduction on *MESP* when liquid hot water was used as pretreatment compared with dilute sulfuric acid pretreatment. Recently, Chen et al.(2015) found a 4.2% increase in *MESP* compared to the 2011 NREL design case (Humbird et al., 2011) when dilute acid pretreatment was replaced by deacetylation and disk refining. Using a modified low-severity dilute acid based pretreatment including disk refining and deacetylation, Tao et al.(2012) found a 13.7% reduction in *MESP* compared to the pretreatment used in the 2011 NREL design case (Humbird et al., 2011). Interestingly, they also analyzed including a solid-liquid separation equipment prior to the liquefaction reactor, allowing the separate processing of the pretreatment liquor and pulp in a configuration similar to C145. Using 20 mg of protein per g of glucan, 20 % of insoluble solids and 120 hours of residence time for the saccharification and fermentation stage, they found an 11% increase in ethanol yield compared to the simultaneous processing of pulp and liquor. Despite the increase in ethanol throughput, the high investment cost in solid-liquid separation equipment leads to a 5.8% increase in *MESP*. In the present work, solid liquid separation after pretreatment allows a reduction on *MESP* compared to the OBC (see C145 and process configurations in **Figure 4**). This opposite result can be explained by a smaller investment cost for the solid liquid separation equipment used in this study, costs that are supported by more accurate information(Sievers et al., 2014) and the reduction of the enzyme dose and insoluble solids loading.

As previously stated, not every process configuration with *MESPs* below the optimized based case is new to the literature. In fact, process configurations C145 and C143 have been previously analyzed by Dutta et al. (2009), using Genencor Spezyme CP (the same enzyme used in the

saccharification model in Scott et al.(2015), but without supplementation of the β-glucosidase activity) at dosages of 30 to 40 mg g^{-1} and diluted acid PCS. Their results show that the best yields and economic results for whole slurry are achieved at 10% total solids, with very low yields at 20%. However, the ethanol titer achieved at 10% total solids is only 2.3% w/v, requiring extra corn stover be fed to the boiler to generate process steam. When xylose was fermented in a separate reactor and the pulp was subject to SSF (a process configuration comparable to C145), the ethanol titer rises to 2.8%. The *MESP* calculated for this case by the authors rises to 1.03 USD kg^{-1}, while for C145 an *MESP* of 61.6 cUSD kg^{-1} was found. The difference in *MESP* rises due to the high enzyme loading used in Dutta et al. (2009), in fact, under identical enzyme dose, the *MESP* of the process configurations C145 reaches 78 cUSD kg^{-1}. Other factors contributing to the high *MESP* in Dutta et al. (2009) are a 27% lower electricity price, taxes, the low ethanol concentration achieved and cost and performance of the solid-liquid separation equipment, which were based on a very preliminary estimation. While for C145, an ethanol titer of 4.1 % *w/v* was calculated, Dutta and coworkers reported a 2.8% *w/v* ethanol content, a low titer that according to their simulation, requires more corn stover to be fed to the boiler for steam generation. However, using the conversions for the saccharification and fermentation stages and the initial solid contents, we calculate a higher ethanol concentration than the one reported in their results.

A second process configuration, equivalent to C143 (**Figure 4**) was analyzed by Dutta et al. (2009), where the liquor separated from the pretreatment reactor is recirculated to the pulp after fermentation. Beyond the expected increase in the titer of ethanol, up to 4.4% *w/v* in Dutta et al. (2009) compared to 6.0 %*w/v* in C143, is interesting to point out that they found that the recirculation of the fermentation liquor produces a decrease in cellulose saccharification yield from 83% to 73%. Dutta and coworkers attribute this decrease in cellulose conversion to "ethanol inhibition or some other inhibitor contained in the beer from xylose fermentation or a

combination of both factors". Process configurations C145 shows an 85% saccharification yield while C143 achieves 76% at their optimal enzyme and solid loadings. Considering that the saccharification model used in this work does not incorporate an inhibitory effect of ethanol, but does include xylose and acetic acid inhibition over the reaction rates of saccharification (Scott et al., 2015), the effects of the latter compounds seem to be sufficient to explain the decrease in cellulose conversion.

The process configurations in the superstructure include continuous saccharification and fermentation reactors. Most of the literature concerning ethanol production from lignocellulosic reports on the use of batch reactors, however, exceptions can be found. Jin el al. (2013) compared the volumetric productivity at similar sugar to ethanol conversions for batch SHCF, SSCF and continuous SSCF (C stands for co-fermentation) using a cascade of five bioreactors, where the first reactor is used as a liquefaction tank. Experiments were performed at 6% total solids of unwashed AFEX^{TM} PCS and 24 mg g^{-1} of Accellerase 1500. The process analyzed by the authors can be mimicked by process configuration C150, under identical enzyme dosages, insoluble solid fractions and total residence time of 52.2 h (distributed in 25 h in R1$_A$, 5.3 h in R1$_B$ and R2$_B$ and 16.6 h in R3$_B$). Under these conditions, an ethanol volumetric productivity equal to 0.66 gL^{-1}h^{-1} and specific ethanol production per mass of enzymes equal to 22.7 kg kg^{-1} was found after solving the NLP representing C150. These values compare with 0.65 gL^{-1}h^{-1} and 21.2 kg/kg found by Jin et al.(2013). The process configurations presented in Figure 4 and **Figure 5** represent promising conceptual designs to be investigated at laboratory and pilot scale. However, they are based in continuous reactors for saccharification and fermentation. Since a batch operation is easier to investigate at these scales, more research is required on how to interpret the process configurations under batch mode, including the effect of moving from continuous operation to batch operation over volumetric productivities and MESP.

Processes including pulp separation were designed according to the results presented by Sievers et al. (2014) where no flocculants were used. In a recent study, Sievers and coworkers at NREL (Sievers et al., 2015) reported a 40-fold increase in filtration flux by using a polyelectrolyte cationic flocculant in the filtration of solids obtained at the end of the enzymatic hydrolysis. Previously, Reye et al. (2011) showed that cationic polyacrylamides (c-PAM) accelerate the cellulase-mediated hydrolysis of bleached softwood Kraft pulp. The mechanism involves the reduction of the negative charge of fibers by c-PAM. As the enzyme is also negatively charged, c-PAM indirectly promotes enzyme binding by reducing charge repulsion between fiber and enzyme. Both results suggest that using cationic polyelectrolytes might simultaneously decrease investment, by augmenting the filtration flux and the hydrolysis rate, and the operational costs by reducing enzyme doses. However, no consistent experimental results are available in the literature for PCS.

In this work, corn stover was chosen as the substrate for ethanol production since enough experimental information was available in the form of kinetic and process models that were consistent with the pretreatment and other auxiliary operations (WWT and CHP). Although the framework can be easily adapted to handle other substrates and operations, obtaining sufficient and consisting experimental information remains a challenge.

The superstructure includes kinetic models for the saccharification and fermentations stages whose parameters were obtained by non-linear fitting to a set of experimental data (Scott et al., 2015). Hence, uncertainty is associated with the parameters in the model and in prices, and thereby, to the economic performance of the saccharification and fermentation operations in the superstructure. A sensitivity analysis was performed considering uncertainty in corn stover, electricity and enzyme prices using an indifference curve analysis (ESI, Figure 6). Results show that, among other process configurations; C69, C145, C131 and C110 can produce a zero-net-

income at an ethanol selling price of 75 cUSD/kg for larger (worst) corn stover and enzyme prices pairs and lower electricity-higher corn stover price pairs. This can be explained by the higher yields achieved at the same enzyme dose for these process configurations compared to the OBC. Regarding the effect of the uncertainty in the parameters of the kinetics models used in the superstructure, a sensitivity analysis was carried out considering the uncertainty intervals presented in Table S1 (ESI). MESP increments up to 20% were found for the OBC while for C145 and C69 the larger increment in MESP was 4%. Moreover, the larger MESP value for C145 or C69 was below the lower MESP found for the OBC under uncertainty (Figures 7 to 9 in ESI). In a subsequent publication, the effect of uncertainty over process design variables and economic indicators will be incorporated into the GDP framework to obtain robust designs.

Conclusions

In this work, a rigorous optimization framework for process synthesis is proposed to find processes for ethanol production from corn stover. Among 150 process configurations, 40 show an improved MESP compared to a well-documented base case and almost all include solid separators. Moreover, 16 of them also show a lower specific capital investment per kg of ethanol produced per year. Some of the resulting process configurations have not been reported and are promising conceptual designs to be investigated at laboratory and pilot scale. Results showed that the process configuration with the lowest *MESP* (61.6 cUSD kg^{-1}) includes solid separators.

Acknowledgements

References

[1] Baliban, R.C., Elia, J.A., Floudas, C.A., 2013. Biomass to liquid transportation fuels (BTL) systems: process synthesis and global optimization framework. Energy Environ. Sci. 6, 267–287.

[2] Brethauer, S., Studer, M.H., 2014. Consolidated bioprocessing of lignocellulose by a microbial consortium. Energy Environ. Sci. 7, 1446.

[3] Bura, R., Lesnicki, G., Saddler, J., Zacchi, G., O, K., 2007. A comparison between simultaneous saccharification and fermentation and separate hydrolysis and fermentation using steam-pretreated corn stover. Process Biochem. 42, 834–839.

[4] Chen, X., Shekiro, J., Pschorn, T., Sabourin, M., Tucker, M.P., Tao, L., 2015. Techno-economic analysis of the deacetylation and disk refining process: characterizing the effect of refining energy and enzyme usage on minimum sugar selling price and minimum ethanol selling price. Biotechnol. Biofuels 8, 173.

[5] Currie, J., Wilson, D.I., 2012. OPTI: Lowering the Barrier Between Open Source Optimizers and the Industrial MATLAB User, in: Foundations of Computer-Aided Process Operations. Savannah, Georgia, USA.

[6] Dale, B.E., 2015. A New Industry Has Been Launched: The Cellulosic Biofuels Ship (Finally) Sails. Biofuels, Bioprod. Biorefining 9, 1–3.

[7] Dale, B.E., Anderson, J.E., Brown, R.C., Csonka, S., Dale, V.H., Herwick, G., Jackson, R.D., Jordan, N., Kaffka, S., Kline, K.L., Lynd, L.R., Malmstrom, C., Ong, R.G., Richard, T.L., Taylor, C., Wang, M.Q., 2014. Take a Closer Look: Biofuels Can Support Environmental, Economic and Social Goals. Environ. Sci. Technol. 48, 7200–7203.

[8] Drud, A., 1985. CONOPT: A GRG code for large sparse dynamic nonlinear optimization problems. Math. Program. 31, 153–191.

[9] Dutta, A., Dowe, N., Ibsen, K.N., Schell, D.J., Aden, A., 2009. An economic comparison of different fermentation configurations to convert corn stover to ethanol using *Z. mobilis* and *Saccharomyces*. Biotechnol. Prog. 26, 64–72.

[10] Gabriel, K.J., El-Halwagi, M.M., 2013. Modeling and optimization of a bioethanol production facility. Clean Technol. Environ. Policy 15, 931–944.

[11] Galbe, M., Zacchi, G., 2007. Pretreatment of Lignocellulosic Materials for Efficient Bioethanol Production 41–65.

[12] Giarola, S., Shah, N., Bezzo, F., 2012. A comprehensive approach to the design of ethanol supply chains including carbon trading effects. Bioresour. Technol. 107, 175–85.

[13] Grossmann, I.E., Ruiz, J.P., 2012. Generalized Disjunctive Programming: A Framework for Formulation and Alternative Algorithms for MINLP Optimization, in: Lee, J., Leyffer, S. (Eds.), Mixed Integer Nonlinear Programming, The IMA Volumes in Mathematics and Its Applications. Springer New York, New York, NY, pp. 93–115.

[14] Hodge, D.B., Karim, M.N., Schell, D.J., McMillan, J.D., 2008. Soluble and insoluble solids contributions to high-solids enzymatic hydrolysis of lignocellulose. Bioresour. Technol. 99, 8940–8.

[15] Humbird, D., Davis, R., Tao, L., Kinchin, C., Hsu, D., Aden, A., Schoen, P., Lukas, J., Olthof, B., Worley, M., Sexton, D., Dudgeon, D., 2011. Process Design and Economics for Biochemical Conversion of Lignocellulosic Biomass to Ethanol. NREL,Golden, Colorado.

[16] Jin, M., Gunawan, C., Balan, V., Yu, X., Dale, B.E., 2013. Continuous SSCF of AFEXTM pretreated corn stover for enhanced ethanol productivity using commercial enzymes and *Saccharomyces cerevisiae* 424A (LNH-ST). Biotechnol. Bioeng. 110, 1302–11.

[17] Leksawasdi, N., Joachimsthal, E., Rogers, P., 2001. Mathematical modelling of ethanol production from glucose/xylose mixtures by recombinant *Zymomonas mobilis*. Biotechnol. Lett. 1087–1093.

[18] Martín, M., 2016. Methodology for solar and wind energy chemical storage facilities design under uncertainty: Methanol production from CO2 and hydrogen. Comput. Chem. Eng. 92, 43–54.

[19] Matthews, L.R., Niziolek, A.M., Onel, O., Pinnaduwage, N., Floudas, C.A., 2015. Biomass to Liquid Transportation Fuels via Biological and Thermochemical Conversion: Process Synthesis and Global Optimization Strategies. Ind. Eng. Chem. Res. acs.iecr.5b03319.

[20] Navarro-Amorós, M.A., Ruiz-Femenia, R., Caballero, J.A., 2014. Integration of modular process simulators under the Generalized Disjunctive Programming framework for the structural flowsheet optimization. Comput. Chem. Eng. 67, 13–25.

[21] Osmani, A., Zhang, J., 2014. Economic and environmental optimization of a large scale sustainable dual feedstock lignocellulosic-based bioethanol supply chain in a stochastic environment. Appl. Energy 114, 572–587.

[22] Raman, R., Grossmann, I.E., 1991. Relation between MILP modelling and logical inference for chemical process synthesis. Comput. Chem. Eng. 15, 73–84.

[23] Reye, J.T., Lu, J., Maxwell, K.E., Banerjee, S., 2011. Enhancement of cellulase catalysis of wood pulp fiber by cationic polyelectrolytes. Biomass and Bioenergy 35, 4887–4891.

[24] Rivera, E.C., Costa, A.C., Atala, D.I.P., Maugeri, F., Maciel, M.R.W., Filho, R.M., 2006. Evaluation of optimization techniques for parameter estimation: Application to ethanol fermentation considering the effect of temperature. Process Biochem. 41, 1682–1687.

[25] Roche, C.M., Dibble, C.J., Knutsen, J.S., Stickel, J.J., Liberatore, M.W., 2009. Particle concentration and yield stress of biomass slurries during enzymatic hydrolysis at high-solids loadings. Biotechnol. Bioeng. 104, 290–300.

[26] Saha, B.C., Nichols, N.N., Qureshi, N., Cotta, M.A., 2011. Comparison of separate hydrolysis and fermentation and simultaneous saccharification and fermentation processes for ethanol production from wheat straw by recombinant *Escherichia coli* strain FBR5. Appl. Microbiol. Biotechnol. 92, 865–74.

[27] Sahinidis, N. V., 1996. BARON: A general purpose global optimization software package. J. Glob. Optim. 8, 201–205.

[28] Scott, F., Conejeros, R., Aroca, G., 2013. Attainable region analysis for continuous production of second generation bioethanol. Biotechnol. Biofuels 6, 171.

[29] Scott, F., Li, M., Williams, D.L., Conejeros, R., Hodge, D.B., Aroca, G., 2015. Corn stover semi-mechanistic enzymatic hydrolysis model with tight parameter confidence intervals for model-based process design and optimization. Bioresour. Technol. 177, 255–65.

[30] Sievers, D.A., Lischeske, J.J., Biddy, M.J., Stickel, J.J., 2015. A low-cost solid-liquid separation process for enzymatically hydrolyzed corn stover slurries. Bioresour. Technol. 187, 37–42.

[31] Sievers, D.A., Tao, L., Schell, D.J., 2014. Performance and techno-economic assessment of several solid–liquid separation technologies for processing dilute-acid pretreated corn stover. Bioresour. Technol. 167, 291–296.

[32] Stickel, J.J., Knutsen, J.S., Liberatore, M.W., Luu, W., Bousfield, D.W., Klingenberg, D.J., Scott, C.T., Root, T.W., Ehrhardt, M.R., Monz, T.O., 2009. Rheology measurements of a biomass slurry: an inter-laboratory study. Rheol. Acta 48, 1005–1015.

[33] Tao, L., Aden, A., Elander, R.T., Pallapolu, V.R., Lee, Y.Y., Garlock, R.J., Balan, V., Dale, B.E., Kim, Y., Mosier, N.S., Ladisch, M.R., Falls, M., Holtzapple, M.T., Sierra, R., Shi, J., Ebrik, M. a, Redmond, T., Yang, B., Wyman, C.E., Hames, B., Thomas, S., Warner, R.E., 2011. Process and technoeconomic analysis of leading pretreatment technologies for lignocellulosic ethanol production using switchgrass. Bioresour. Technol. 102, 11105–14.

[34] Tao, L., Chen, X., Aden, A., Kuhn, E., Himmel, M.E., Tucker, M., Franden, M.A. a, Zhang, M., Johnson, D.K., Dowe, N., Elander, R.T., 2012. Improved ethanol yield and reduced minimum ethanol selling price (MESP) by modifying low severity dilute acid pretreatment with deacetylation and mechanical refining: 2) Techno-economic analysis. Biotechnol. Biofuels 5, 69.

[35] Teugjas, H., Väljamäe, P., 2013. Product inhibition of cellulases studied with 14C-labeled cellulose substrates. Biotechnol. Biofuels 6, 104.

[36] Thek, G., Obernberger, I., 2004. Wood pellet production costs under Austrian and in comparison to Swedish framework conditions. Biomass and Bioenergy 27, 671–693.

[37] Tsakalova, M., Lin, T.C., Yang, A., Kokossis, A.C., 2015. A decision support environment for the high-throughput model-based screening and integration of biomass processing paths. Ind. Crops Prod. 75, 103–113.

[38] Türkay, M., Grossmann, I.E., 1996. Logic-based MINLP algorithms for the optimal synthesis of process networks. Comput. Chem. Eng. 20, 959–978.

[39] Wächter, A., Biegler, L.T., 2006. On the implementation of an interior-point filter line-search algorithm for large-scale nonlinear programming. Math. Program. 106, 25–57.

[40] Whistance, J., Thompson, W., Meyer, S., 2017. Interactions between California's Low Carbon Fuel Standard and the National Renewable Fuel Standard. Energy Policy 101, 447–455.

[41] Williams, H.P., 1999. Building Integer Programming Models I, in: Model Building in Mathematical Programming. John Wiley & Sons Ltd, Midsomer Norton, pp. 154–186.

[42] You, F., Tao, L., Graziano, D.J., Snyder, S.W., 2012. Optimal design of sustainable cellulosic biofuel supply chains: Multiobjective optimization coupled with life cycle assessment and input-output analysis. AIChE J. 58, 1157–1180.
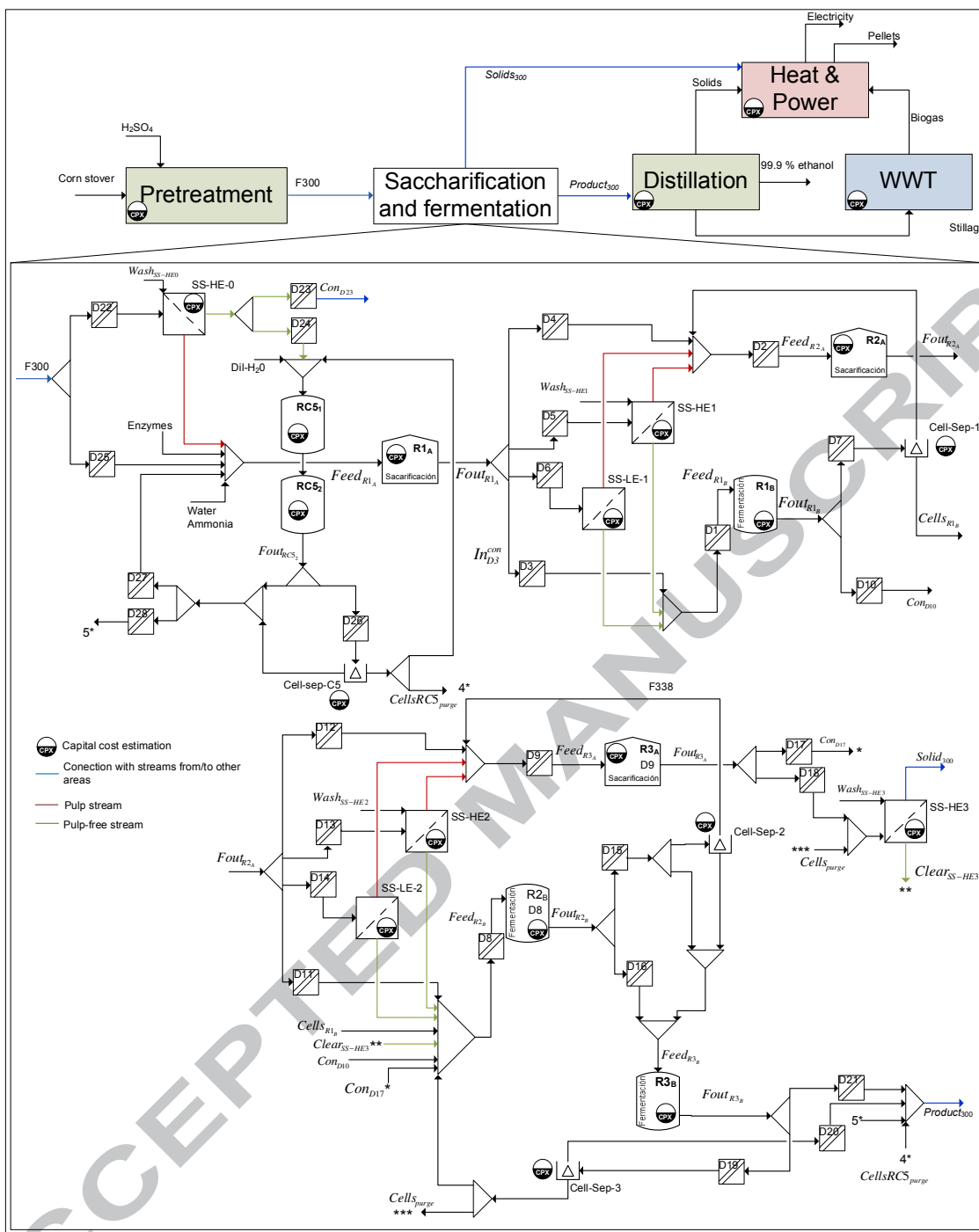
Figure 1: Conceptual design of the superstructure for ethanol production from corn stover including process alternatives in the saccharification and fermentation stage.
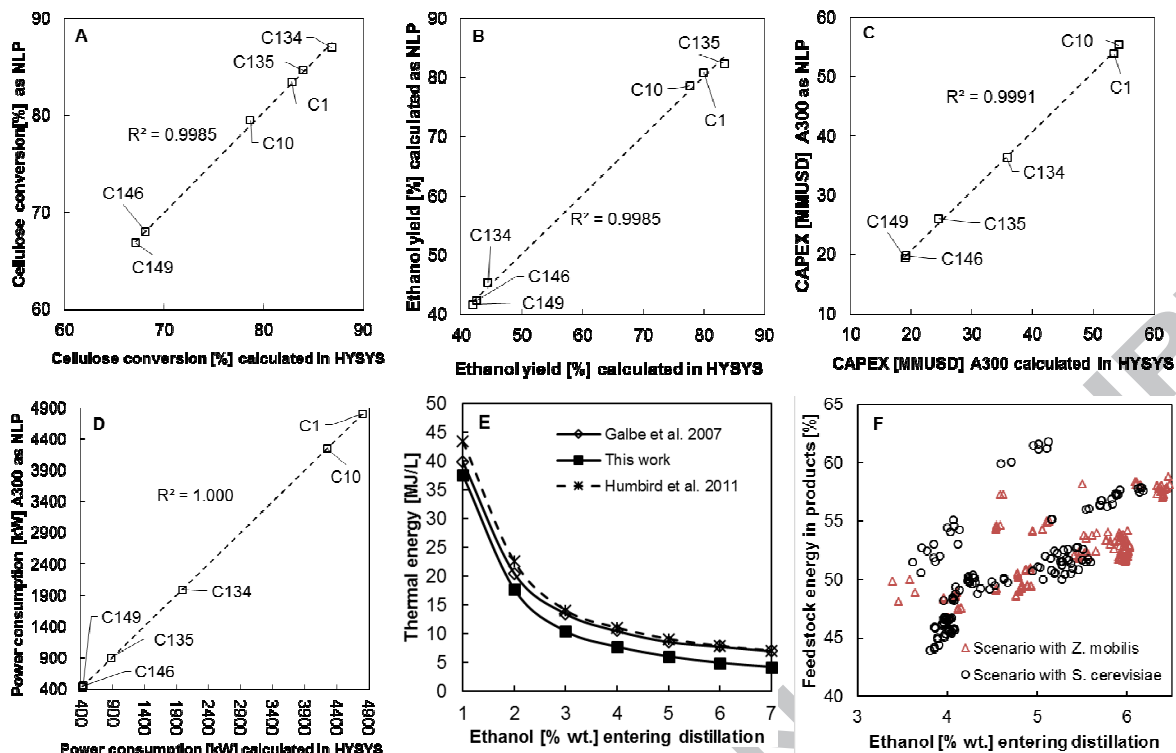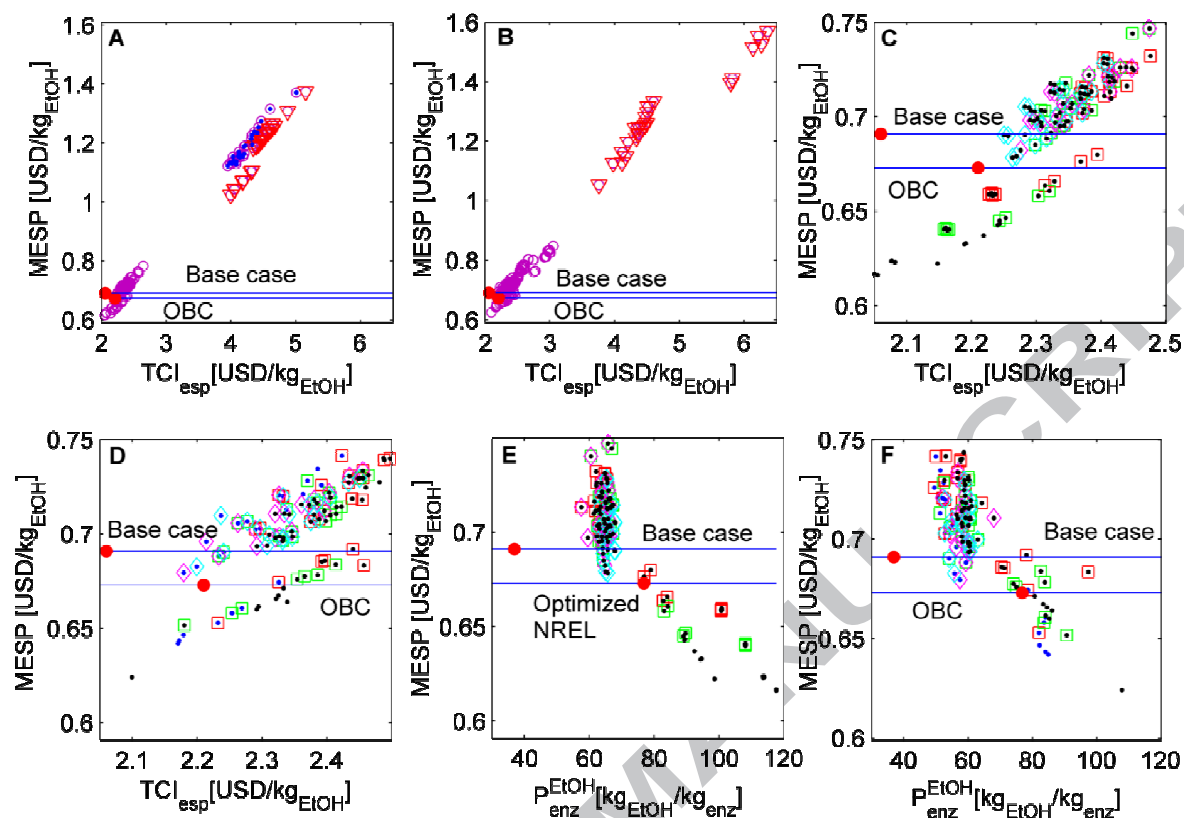
Figure 2: Comparison between key process indicators calculated in HYSYS and calculated by the NLP representation of the superstructure.

Figure 3: Results from the non-linear optimization of every process in the superstructure for two scenarios. Panels A, C and E show results for the scenario where *S. cerevisiae* is used in reactors R1$_B$ to R3$_B$. Panels B, D and F display results for the scenario where *Z. mobilis* is used in every fermentor of the network. ● solid separation after pretreatment (D22 is active), ●: no solid separation in pretreatment (D25 is active), ● Base case process configuration, □: high efficiency pulp separator (D5 active), □: low efficiency pulp separator (D6 active), ◊: high efficiency pulp separator (D13 active), ◊: low efficiency pulp separator (D14 active), ▽ : pretreatment liquor (rich in xylose) is sent to biogas production (D23 is active).
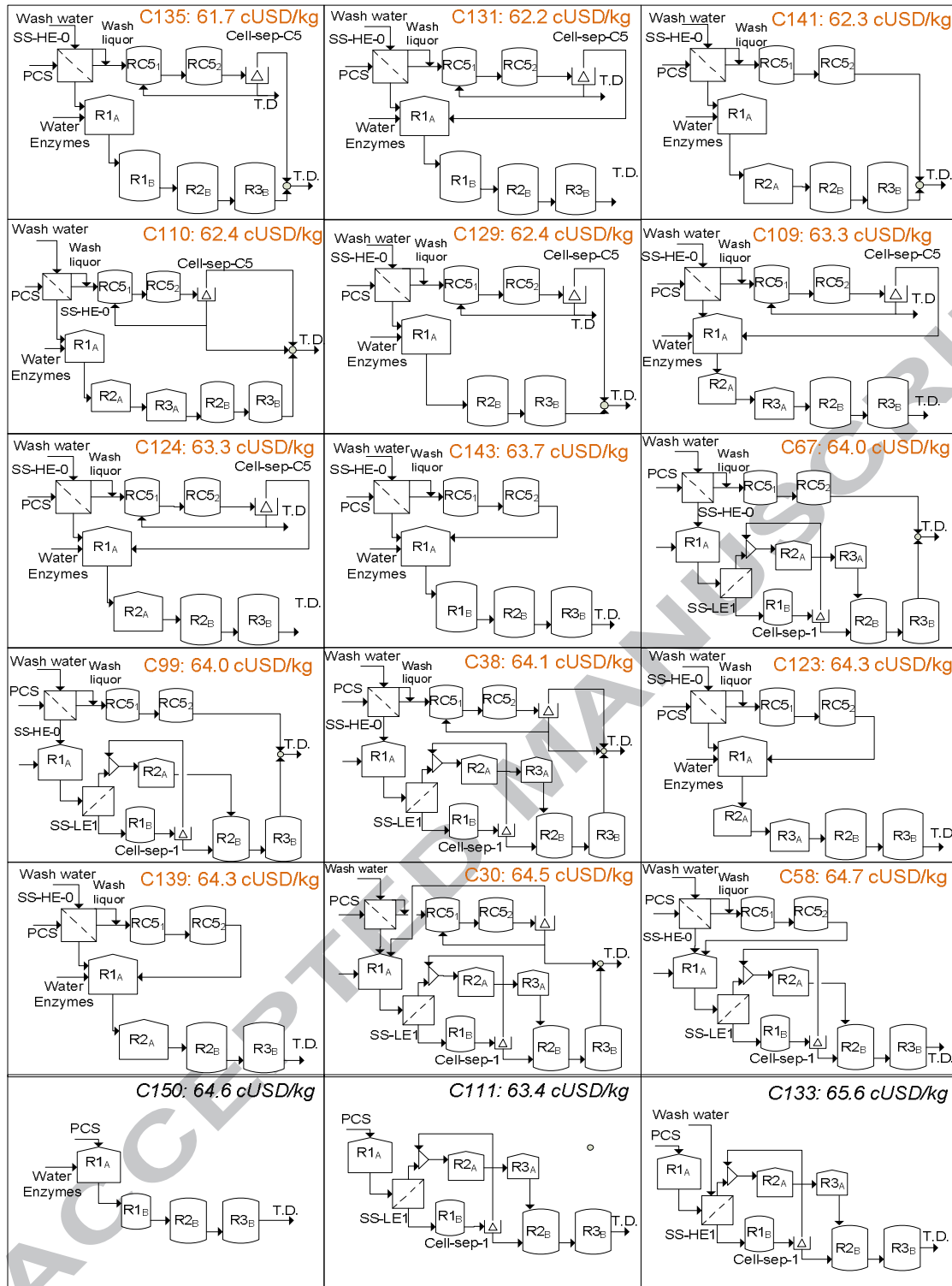
Figure 4. *MESP* and simplified flow diagram of the process configuration showing *MESP* values below 65 cUSD/kg (except **C133**). Process configurations C150, C111 and C133 use *Z. mobilis* in each fermentor, the remaining proccess configurations use *S. cerevisiae* in reactors R1$_B$ to R3$_B$. T.D. indicates streams going to distillation.
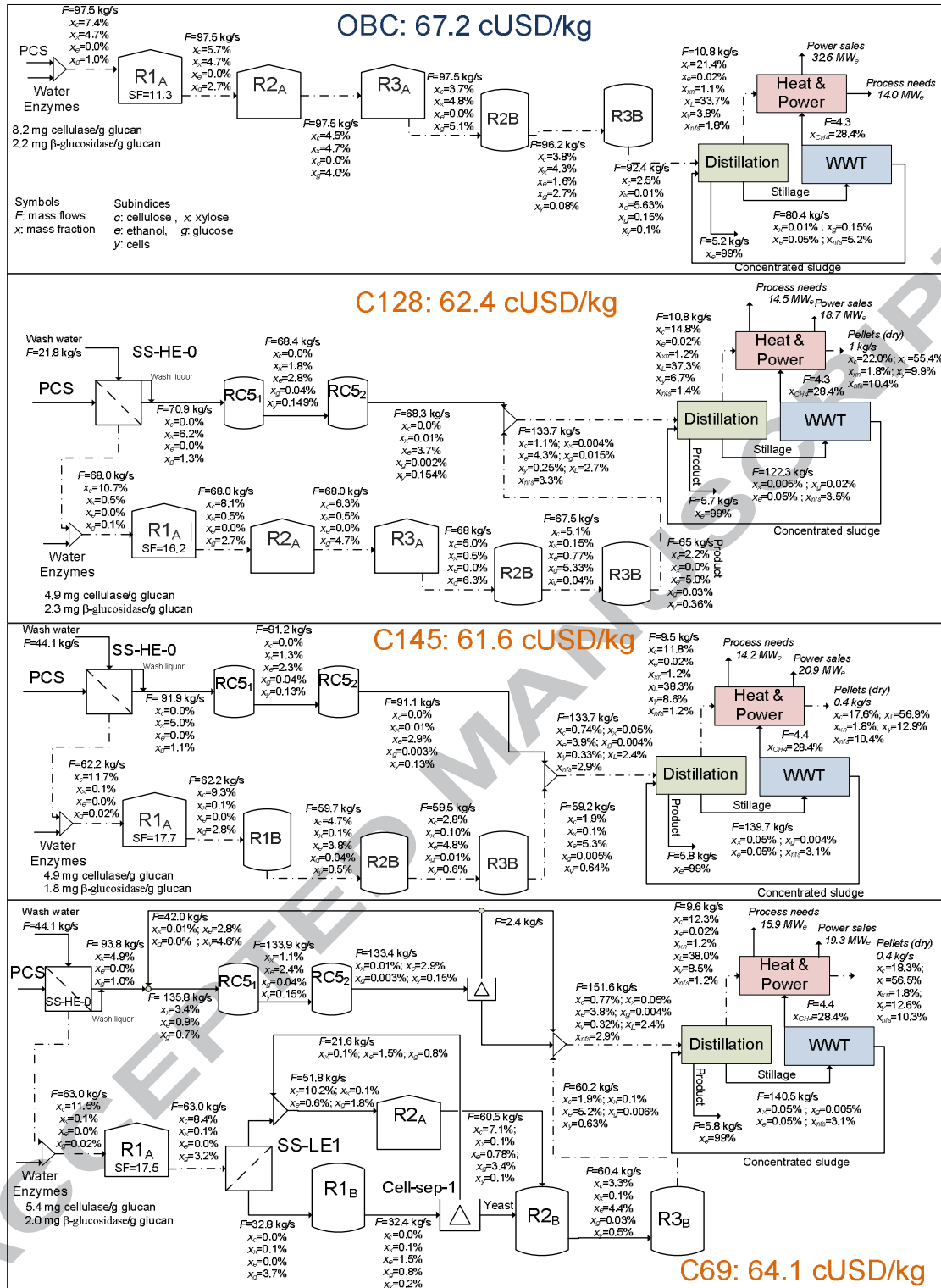
Figure 5: *MESP* and simplified mass balances for selected process configurations. Processes OCB and C128 use *Z. mobilis* in every fermentor. C145 and C69 use *S. cerevisiae* in $R1_B$ to $R3_B$.

34

Table 1: Investment per process area, operating cost, sales, economic and energetic indicators for selected process configurations.

	Units	OBC	C145	C69	C128	C131	C111
Installed Equipment costs and total investment							
Saccharification & fermentation	MMUSD	23.2	28.4	34.5	28.7	31.9	26.5
Distillation & solids separation	MMUSD	18.0	18.5	18.6	18.5	18.2	17.4
Heat & power	MMUSD	58.4	55.0	55.2	53.2	50.2	47.5
Wastewater treatment	MMUSD	47.3	53.0	53.0	51.1	48.6	45.2
Total direct cost	MMUSD	204.7	214.6	222.0	212.2	211.6	199.7
Total capital investment	MMUSD	345.8	362.4	374.9	358.3	357.4	337.3
Operating costs							
Enzymes	MMUSD	-9.6	-6.4	-6.8	-6.7	-7.2	-9.5
Corn stover	MMUSD	-44.7	-44.7	-44.7	-44.7	-44.7	-44.7
Chemicals, maintenance, labor and insurance	MMUSD	-20.7	-20.9	-21.3	-20.8	-20.6	-19.9
Sales [MMUSD]							
Ethanol	MMUSD	105.0	108.3	111.2	106.5	103.6	99.0
Electricity	MMUSD	15.1	9.6	8.9	8.6	6.9	5.1
Pellets	MMUSD	0.0	1.3	1.4	3.7	8.4	13.9
Economic indicators							
Payback (based in EBITDA with ethanol at 75 cUSD/kg)	Years	6.17	5.36	5.70	5.34	5.39	5.63
Ethanol price for ROI=20%	USD/kg	0.83	0.78	0.80	0.78	0.78	0.80
MESP with 20% tax (calculated with DCFOR)	USD/kg	0.70	0.62	0.64	0.62	0.62	0.64
Energy indicators							
Specific thermal energy per unit of ethanol	kJ/kg	10270	14892	15053	138030	12170	11119
Specific electric energy per unit of ethanol	kJ_e/kg	2708	2479	2789	2551	2754	3245
Total energy in products	%	46.9	50.1	49.7	52.6	57.7	62.4

35

Superstructure modeling
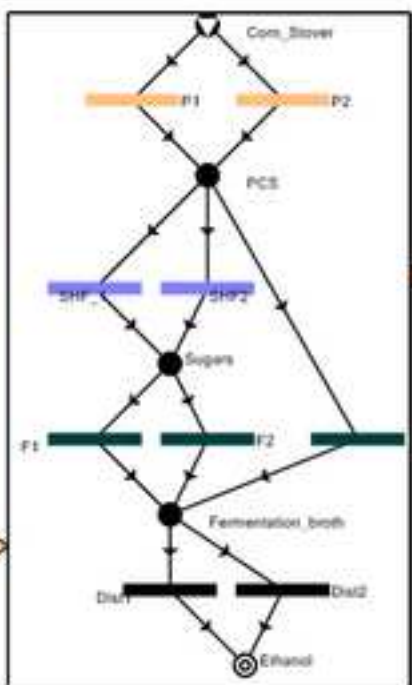
Kinetic models of saccharification and fermentation

Ranking of improved MESP process configurations
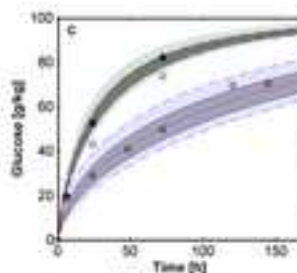
$$\min_{x,Y} f(x)$$

s.t.

$Ax \leq b$

$g(x) \leq 0$

$h(x) = 0$

$$\begin{bmatrix} Y_i \\ A_i x_i \leq b_i \\ g_i(x_i) \leq 0 \\ h_i(x_i) = 0 \end{bmatrix} \vee \begin{bmatrix} \neg Y_i \\ x_i = 0 \end{bmatrix} i \in K$$

$\Omega(Y) = True$

$x_i \subset x;$

Topology and operational optimization
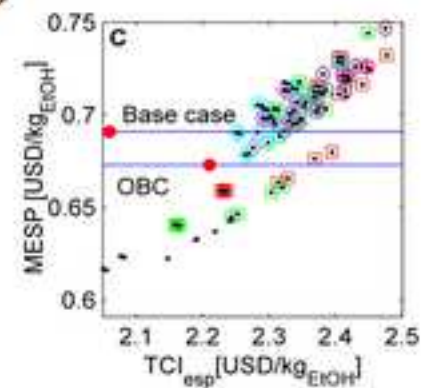
4 Highlights

- An optimization framework for process design of ethanol plants is presented
- 150 different process configurations are compared and analyzed
- New process configurations outperform the NRELs base case
- Lower MESPs were found when solid-liquid separators are included
- Energy in products ranges from 44% to 62.4% of the energy in corn stover